Thermochimica Acta 503–504 (2010) 115–120

Contents lists available at ScienceDirect

Thermochimica Acta

journal homepage: www.elsevier.com/locate/tca

Prediction of phase equilibria and thermal analysis in the Bi–Cu–Pb ternary system

Dragan Manasijević[a], Aleksandra Mitovski[a,*], Duško Minić[b], Dragana Živković[a], Saša Marjanović[a], Radiša Todorović[c], Ljubiša Balanović[a]

[a] University of Belgrade, Technical Faculty, VJ 12, 19210 Bor, Serbia
[b] University of Pristina, Faculty of Technical Sciences, 38220 Kosovska Mitrovica, Serbia
[c] Institute of Mining and Metallurgy, Zeleni Bulevar 35, 19210 Bor, Serbia

ARTICLE INFO

Article history:
Received 21 January 2010
Received in revised form 1 March 2010
Accepted 5 March 2010
Available online 25 March 2010

Keywords:
Bi–Cu–Pb ternary system
Phase diagram
Thermodynamic prediction
Thermal analysis

ABSTRACT

The knowledge about phase diagram of the Bi–Cu–Pb ternary system is of importance in development of copper–lead based bearing materials, soldering and in refining of copper and lead.

In this work, the phase diagram of the Bi–Cu–Pb ternary system was calculated by the CALPHAD method using binary thermodynamic parameters included in the COST 531 database. The results include liquidus projection, invariant equilibria and three vertical sections with molar ratio Cu:Pb = 1, Cu:Pb = 1:3 and Bi:Cu = 1. Alloys, with compositions along three predicted vertical sections, were measured using differential scanning calorimetry (DSC). The experimentally determined phase transition temperatures were compared with calculated results and good mutual agreement was noticed.

1. Introduction

Copper–lead based alloys are frequently used as bearing materials. Since lead is practically insoluble in copper, a cast copper–lead microstructure consists of lead pockets in a copper matrix. These pockets of lead serve as reservoirs for maintaining a continuous lead film on the bearing surface. By adding bismuth in a copper–lead based bearing alloy it becomes possible to obtain excellent corrosion resistance without impairing the conformability and seizure resistance of the bearing material in comparison with the conventional copper–lead based bearing alloys. Phase relations in Bi–Cu–Pb ternary system are of importance in soldering and refining operations, also. Thus, knowledge about phase diagram of ternary Bi–Cu–Pb system is of interest from scientific and technological points of view.

In this paper, the phase transition temperatures of the Bi–Cu–Pb ternary system are investigated using differential scanning calorimetry (DSC). Experimentally obtained results are compared with the results of thermodynamic binary-based prediction, based on the 4.4 SGTE values of Gibbs energies for pure elements [1] and thermodynamic binary data included in the COST 531 thermodynamic database [2].

2. Experimental

The samples with a total mass of about 2 g were prepared by induction melting of pure metals (purity higher than 99.99%) under argon atmosphere. The total mass losses of the prepared ingots were less than 0.5 mass%. The alloy samples were then encapsulated in quarts tubes under vacuum, homogenized at 800 °C for several hours and slowly cooled to room temperature. Homogeneity of samples was examined before DSC measurements using scanning electron microscopy (SEM) analysis.

The DSC measurements were performed on a SDT Q600 (TA Instruments). Alumina crucibles were used and measurements were performed under flowing argon atmosphere. Samples weighing between 70 and 100 mg were investigated using the heating rate of 5 °C/min.

3. Thermodynamic models and crystallographic data

Phase diagram of the Bi–Cu–Pb ternary system was calculated by the calculation of phase diagrams (CALPHAD) method [3], using optimized thermodynamic parameters for constitutive binary systems only. The basic mathematical method used for the calculation of phase equilibria is a constrained minimisation of Gibbs energy for a given temperature, pressure and overall composition. This approach is common for all currently available software packages for the modeling of thermodynamic properties and phase diagrams of multicomponent systems.

* Corresponding author at: Department of Metallurgical Engineering, University of Belgrade, Technical Faculty, VJ 12, 19210 Bor, Serbia. Tel.: +381 30 424555; fax: +381 30 424555.
E-mail address: amitovski@tf.bor.ac.rs (A. Mitovski).

0040-6031/$ – see front matter © 2010 Elsevier B.V. All rights reserved.
doi:10.1016/j.tca.2010.03.018

The molar Gibbs energy of a phase ϕ can be considered as the sum of a number of different contributions:

$$G_m^\phi = G_{ref}^\phi + G_{id}^\phi + G_E^\phi + G_{mag}^\phi + G_P^\phi + \ldots \quad (1)$$

where G_{ref}^ϕ is the weighted sum of the molar Gibbs energy of the system constituents i (elements, species, compounds, etc.) of the phase ϕ relative to the chosen reference state (typically the Stable Element Reference state—SER),

$$G_{ref}^\phi = \sum_{i=1}^{n} x_i \cdot {}^oG_i^\phi \quad (2)$$

and its temperature dependence is given by:

$$G(T) = a + bT + cT\ \ln(T) + \sum_i d_i T^n \quad (3)$$

where a–d_i are adjustable coefficients.

There is also a contribution to the Gibbs energy from ideal random mixing of the constituents on the crystal lattice, denoted G_{id}^ϕ,

$$G_{id}^\phi = RT\sum_{i=1}^{n} x_i \cdot \ln(x_i), \quad i = 1, \ldots, n \quad (4)$$

for an n-constituent system.

G_E^ϕ is the excess Gibbs energy, which describes the influence of non-ideal mixing behaviour on the thermodynamic properties of a solution phase and is given by the Muggianu extension of the Redlich–Kister formalism [4,5]:

$$G_E^\phi = \sum_{\substack{i,j=1\\ i\neq j}}^{n} x_i x_j \sum_{z=0}^{m} L_{i,j}^z \left(x_i - x_j\right)^z + \sum_{\substack{i,j,k=1\\ i\neq j\neq k}}^{n} x_i x_j x_k L_{i,j,k} \quad (5)$$

where the interaction parameters, describing the mutual interaction among constituents i, j and k, are denoted as L.

The liquid phase and solid solution phases are modeled in this way, but more complex phases, such as intermetallic compounds, are usually modeled using the compound energy formalism [6].

Additional terms may be necessary for the proper description of the Gibbs energy from Eq. (1). G_{mag}^ϕ in Eq. (1) is the magnetic contribution and G_P^ϕ is the pressure term.

The magnetic contribution to the thermodynamic properties has been defined by Hillert and Jarl [7] following the work of Inden [8,9]. According to Hillert and Jarl the contribution to the Gibbs energy is given by:

$$G_{mag}^\phi = RT\ \ln(B_0 + 1)g(\tau) \quad (6)$$

where τ is T/T^*, T^* is the critical temperature (the Curie temperature, T_C, for ferromagnetic materials or the Neel temperature, T_N, for antiferromagnetic materials) and B_0 is the average magnetic moment per atom. $g(\tau)$ is given by:

$$g(\tau) = 1 - \frac{[(79\tau^{-1}/140p) + (474/497)((1/p) - 1)((\tau^3/6) + (\tau^9/135) + (\tau^{15}/600))]}{D}, \quad \tau \leq 1$$

$$g(\tau) = \frac{-[(\tau^{-5}/10) + (\tau^{-15}/315) + (\tau^{-25}/1500)]}{D}, \quad \tau > 1$$

where

$$D = \frac{518}{1125} + \frac{11692}{15975}\left(\frac{1}{p} - 1\right) \quad (7)$$

The value of p, which can be thought of as the fraction of the magnetic enthalpy absorbed above the critical temperature, depends on the structure. For the simple BCC_A2 phase $p = 0.40$ while for other common phases encountered $p = 0.28$.

Table 1
Considered phases, their crystallographic data and database names [12].

Common name	Thermodynamic database name	Strukturbericht designation	Pearson symbol
Liquid	LIQUID	–	–
(Cu) (Pb)	FCC_A1	*A1*	*cF4*
(Bi)	RHOMBO_A7	*A7*	*hR2*
ζ	HCP_A3	*A3*	*hP2*

The pressure dependence for condensed phases is expressed in the form of the Murnaghan equation [10,11]:

$$G_P^\phi = \frac{A\ \exp\left(a_0T + a_1T^2/2 + a_2T^3/3 + a_3T^{-1}\right)}{\left(K_0 + K_1T + K_2T^2\right)(n-1)} \times \left[\left(1 + nP\left(K_0 + K_1T + K_2T^2\right)\right)^{1-1/n} - 1\right] \quad (8)$$

where A, a_0, a_1, a_2, a_3, K_0, K_1, K_2 and n are constants for the particular element and phase and P is the pressure. However, pressure dependence for condensed systems at normal pressures is usually ignored.

The phases from constitutive binary subsystems considered for thermodynamic binary-based prediction with their crystallographic data are listed in Table 1.

The Version 4.4 of the SGTE Unary Database (Scientific Group Thermodata Europe) of phase stabilities for stable and metastable states of pure elements [1] was used.

Thermodynamic data for the Bi–Cu system were taken from Ref. [13], for the Bi–Pb system were published in Ref. [14], and thermodynamic data for the system Cu–Pb were taken from Ref. [15]. All this data are included in the COST 531 Database for Lead Free Solders [2].

Optimized thermodynamic binary parameters used in this study are given in Table 2.

4. Literature data

4.1. Binary systems

4.1.1. Bi–Cu system

The Bi–Cu system is a simple eutectic system showing no solubility of Cu in solid Bi. The solubility of Bi in solid Cu was determined in the temperature range from 600 to 1040 °C by Chang et al. [16] and the maximum solubility was found to be 0.0207 at.% at 975 °C. Calculated phase diagram, based on thermodynamic description from Refs. [2,13], is given in Fig. 1.

4.1.2. Bi–Pb system

The Bi–Pb system exhibits both a eutectic reaction and the peritectic formation of an intermetallic ξ phase. A considerable amount of Bi may dissolve in crystalline Pb but there is negligible solubility for Pb in crystalline Bi. The thermodynamic description used in this study is from Refs. [2,14]. Calculated phase diagram of the Bi–Pb binary system is shown in Fig. 2.

4.1.3. Cu–Pb system

The most prominent feature of the Cu–Pb phase diagram is the monotectic reaction leading to phase separation in the liquid phase. There is negligible mutual solid solubility between Cu and Pb. The thermodynamic dataset used here was taken from [2,15]. As Cu and

Table 2
Optimized thermodynamic parameters for constitutive binaries used in this study.

Phase and thermodynamic model	Thermodynamic parameters	Reference
LIQUID (Bi, Cu, Pb)	${}^{0}L^{\mathrm{LIQUID}}_{\mathrm{Bi,Cu}} = 20747.5 - 5.85T$	[2,13]
	${}^{1}L^{\mathrm{LIQUID}}_{\mathrm{Bi,Cu}} = -4925 + 2.55T$	[2,13]
	${}^{2}L^{\mathrm{LIQUID}}_{\mathrm{Bi,Cu}} = 4387.5 - 2.3T$	[2,13]
	${}^{0}L^{\mathrm{LIQUID}}_{\mathrm{Bi,Pb}} = -4330.3 - 2.0421T + 0.06542T\ln(T)$	[2,14]
	${}^{1}L^{\mathrm{LIQUID}}_{\mathrm{Bi,Pb}} = 1.53 - 1.02298T$	[2,14]
	${}^{2}L^{\mathrm{LIQUID}}_{\mathrm{Bi,Pb}} = 896.7 - 1.2644T$	[2,14]
	${}^{0}L^{\mathrm{LIQUID}}_{\mathrm{Cu,Pb}} = 27190.2 - 4.21329T$	[2,15]
	${}^{1}L^{\mathrm{LIQUID}}_{\mathrm{Cu,Pb}} = 2229.2 - 0.53584T$	[2,15]
	${}^{2}L^{\mathrm{LIQUID}}_{\mathrm{Cu,Pb}} = -7029.2 + 6.48832T$	[2,15]
	${}^{3}L^{\mathrm{LIQUID}}_{\mathrm{Cu,Pb}} = -7397.6 + 5.07992T$	[2,15]
FCC_A1 $(\mathrm{Bi,Cu,Pb})_1(\mathrm{Va})_1$	${}^{0}L^{\mathrm{FCC\_A1}}_{\mathrm{Bi,Cu:Va}} = 50T$	[2,13]
	${}^{0}L^{\mathrm{FCC\_A1}}_{\mathrm{Bi,Pb:Va}} = -2852.75 - 3.5832T$	[2,14]
	${}^{0}L^{\mathrm{FCC\_A1}}_{\mathrm{Cu,Pb:Va}} = 74090.9 - 24.69707T$	[2,15]
RHOMBO_A7 (Bi,Pb)	${}^{0}L^{\mathrm{RHOMBO\_A7}}_{\mathrm{Bi,Pb}} = 3461.59 + 45.2234T$	[2,14]
HCP_A3 $(\mathrm{Bi,Cu,Pb})_1(\mathrm{Va})_{0.5}$	${}^{0}L^{\mathrm{HCP\_A3}}_{\mathrm{Bi,Cu:Va}} = 50T$	[2]
	${}^{0}L^{\mathrm{HCP\_A3}}_{\mathrm{Bi,Pb:Va}} = -4441.67 - 7.4411T$	[2,14]
	${}^{1}L^{\mathrm{HCP\_A3}}_{\mathrm{Bi,Pb:Va}} = 1725.26 - 4.022T$	[2,14]
	${}^{0}L^{\mathrm{HCP\_A3}}_{\mathrm{Cu,Pb:Va}} = 74090.9 - 24.69707T$	[2]

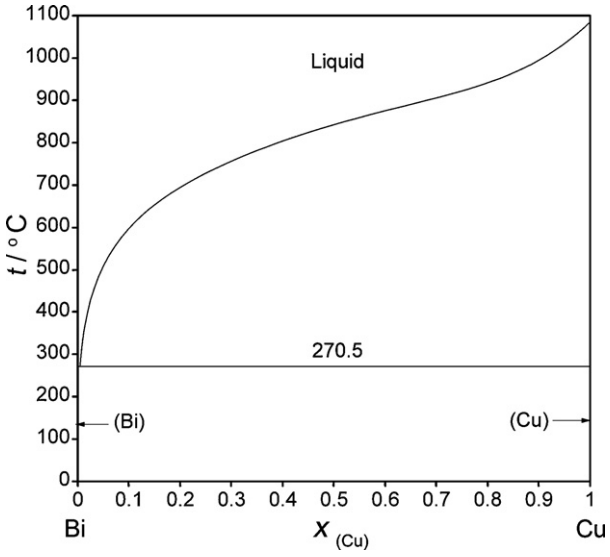

Fig. 1. Calculated phase diagram of the Bi–Cu binary system.

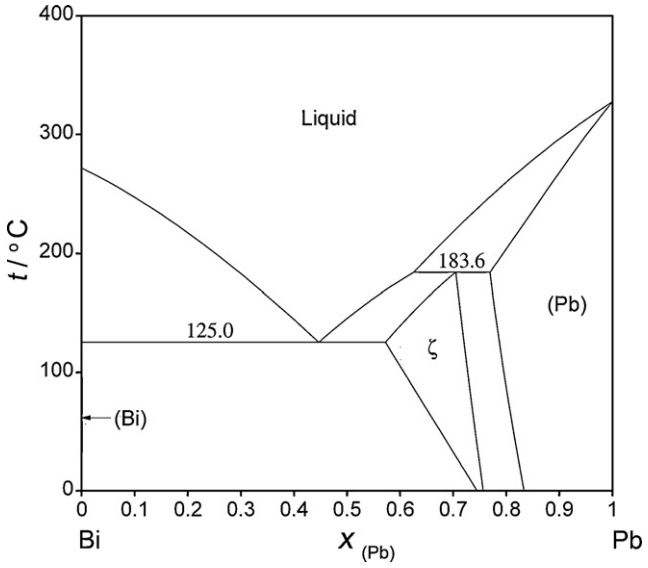

Fig. 2. Calculated phase diagram of the Bi–Pb binary system.

Pb have the same crystal structure, they have been treated with a single Gibbs energy expression. Calculated phase diagram of the Cu–Pb binary system is shown in Fig. 3.

4.2. Bi–Cu–Pb ternary system

The extrapolated liquidus projection and invariant equilibria of ternary Bi–Cu–Pb ternary system is presented by Kattner [17]. It seems that there are no published experimental results about phase relations in the Bi–Cu–Pb ternary system.

5. Results and discussion

Only binary thermodynamic descriptions are known in the system Bi–Cu–Pb. Ternary parameters are not available. Therefore the calculation of the Bi–Cu–Pb phase diagram was performed only on the basis of binary thermodynamic data included in the COST 531 database [2]. Ternary phase diagram calculated in this way represents predicted or extrapolated phase diagram and it does not have a capability to evaluate any new ternary phase or solubility of third element in any binary phase. Thus the correctness of the predicted phase diagram should always be checked by the carefully planned experimental program. The experimental part in this work includes DSC measurements of the selected Bi–Cu–Pb ternary alloys in order to investigate the accuracy of calculated temperatures of invariant reactions and liquidus surface.

5.1. Predicted liquidus projection and invariant equilibria of the Bi–Cu–Pb ternary system

The liquidus projection of the Bi–Cu–Pb ternary system is calculated and plotted in Fig. 4. Two invariant reactions: ternary eutectic

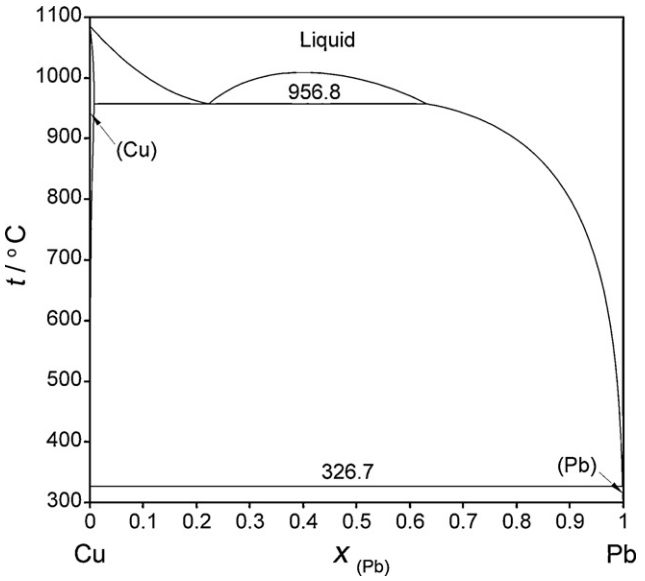

Fig. 3. Calculated phase diagram of the Cu–Pb binary system.

reaction at 125.0 °C and ternary quasi-peritectic reaction at 183.5 °C are predicted in this ternary system. Liquid miscibility gap and four primary crystallization regions (Cu-based solid solution and very narrow (Bi), ξ and Pb-based solid solution) are identified (Fig. 5).The calculated temperatures of ternary invariant reactions and the compositions of the corresponding phases are listed in Table 3. Predicted results from this work are in good agreement with those published in Ref. [17].

5.2. Experimental study of phase transition temperatures

In order to experimentally study the phase transition temperatures of the Bi–Cu–Pb ternary system, the alloys with overall compositions alongside three chosen vertical sections with molar ratio Cu:Pb = 1, Cu:Pb = 1/3 and Bi:Cu = 1 were investigated by DSC. The analysis of DSC measurements was performed during the heating of samples. Temperatures of phase transitions were read using

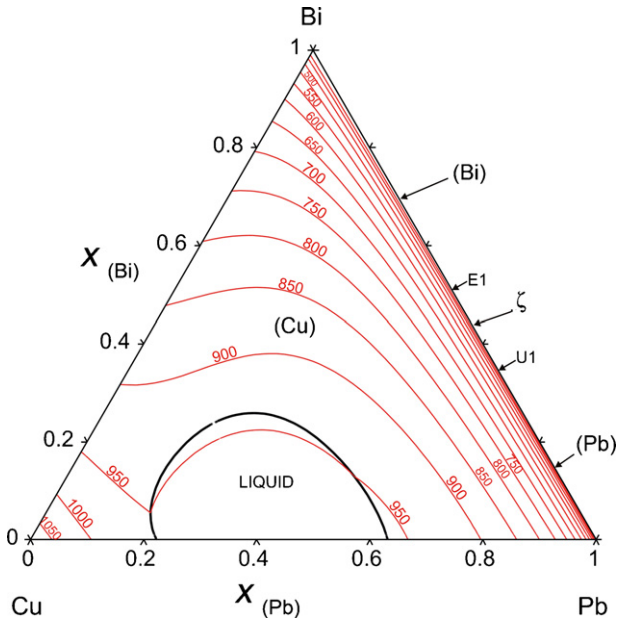

Fig. 4. The predicted liquidus projection of the Bi–Cu–Pb ternary system.

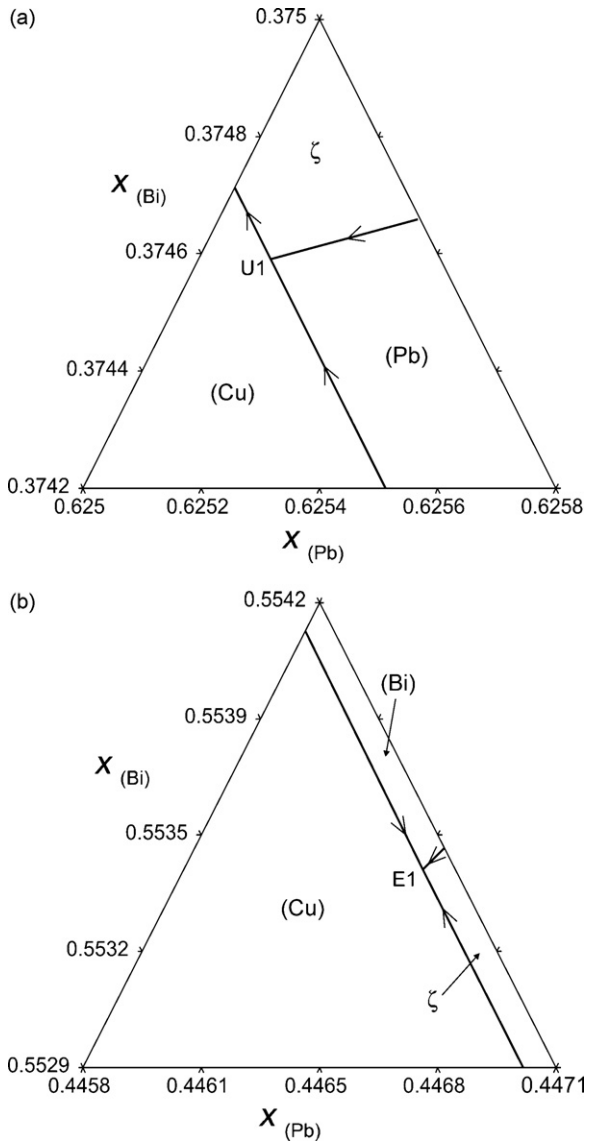

Fig. 5. Magnified views of the liquidus projection of the Bi–Cu–Pb ternary system in the vicinity of two predicted invariant points: (a) U_1 invariant point and (b) E_1 invariant point.

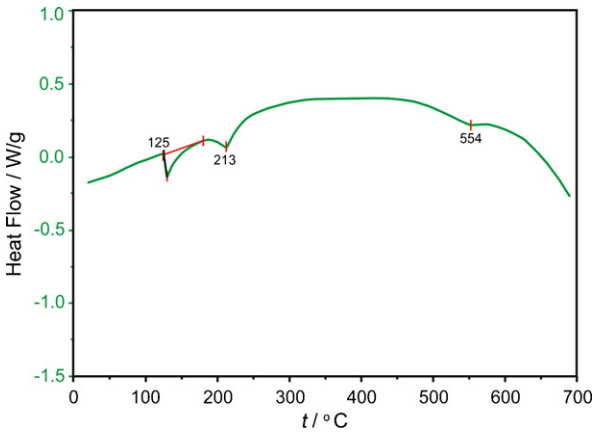

Fig. 6. DSC curve for the Bi80Cu5Pb15 sample with the determined phase transition temperatures.

Table 3
Calculated invariant equilibria in the Bi–Cu–Pb ternary system from this work and Ref. [17].

Reaction	Type	Temperature (°C)		Phase	Composition					
		This work	Ref. [17]		This work			Ref. [17]		
					x_{Bi}	x_{Cu}	x_{Pb}	x_{Bi}	x_{Cu}	x_{Pb}
$L + (Pb) \leftrightarrow (Cu) + \xi$	U_1	183.5	184.9	Liquid	0.375	0	0.625	0.359	0	0.641
				(Pb)	0.231	0	0.769	0.231	0	0.769
				(Cu)	0	1	0	0	1	0
				ξ	0.295	0	0.705	0.278	0	0.722
$L \leftrightarrow (Bi) + \xi + (Cu)$	E_1	125.0	125.9	Liquid	0.553	0	0.446	0.553	0	0.447
				(Bi)	1	0	0	0.995	0	0.005
				ξ	0.428	0	0.572	0.419	0	0.581
				(Cu)	0	1	0	0	1	0

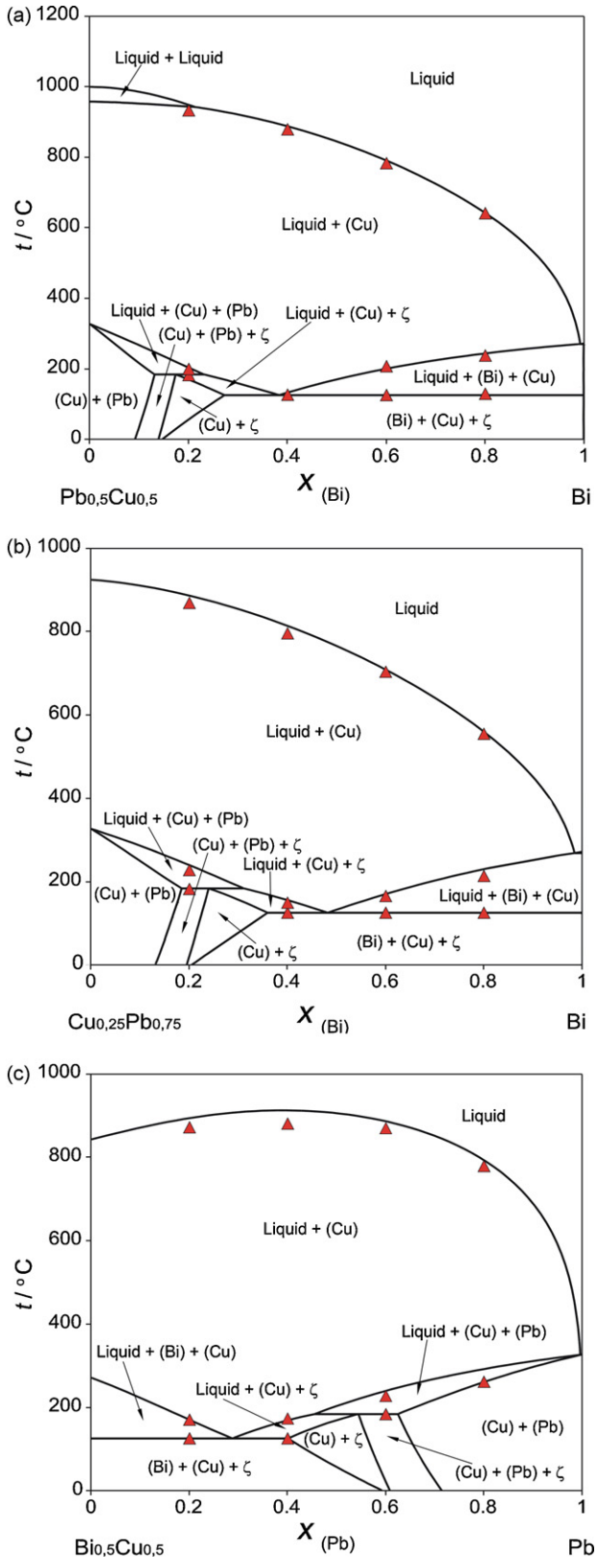

Fig. 7. Predicted vertical sections of the Bi–Cu–Pb ternary system compared with DSC results (triangle) from the present study: (a) Cu:Pb = 1, (b) Cu:Pb = 1:3, and (c) Cu:Bi = 1.

Table 4
Phase transition temperatures for the investigated alloys of the Bi–Cu–Pb ternary system from the present DSC measurements.

Sample composition [at.%]	Phase transition temperature [°C]		
	Invariant reaction	Other transition	Liquidus
Bi20Cu40Pb40	183	199	932
Bi40Cu30Pb30	126	–	878
Bi60Cu20Pb20	125	207	782
Bi80Cu10Pb10	125	237	640
Bi20Cu20Pb60	182	227	868
Bi40Cu15Pb45	125	149	795
Bi60Cu10Pb30	125	165	703
Bi80Cu5Pb15	125	213	554
Bi40Cu40Pb20	125	170	871
Bi30Cu30Pb40	125	172	880
Bi10Cu10Pb80	–	261	778

software delivered with the instrument. Predicted phase equilibrium data were used as help to interpret obtained DSC results. The temperatures of invariant phase transitions were taken from the extrapolated onset on heating. The other phase transition temperatures were taken from the peak temperature. Fig. 6 shows characteristic DSC heating curve. The onset temperature of the first peak is in excellent agreement with the calculated ternary eutectic reaction at 125 °C (Table 3). The temperatures of the last two peaks correspond to the monovariant transition and melting of the sample.

Calculated vertical sections with phase transition temperatures from the present DSC measurements are plotted in Fig. 7(a)–(c). The calculated vertical sections are in good agreement with experimental results.

Thermal analysis results given in the Table 4 show good agreement with the calculated temperatures of two invariant reactions: ternary eutectic reaction at 125.0 °C and ternary quasi-peritectic reaction at 183.5 °C. From Fig. 7(a)–(c) one can observe that the calculated liquidus temperatures also show agreement with experimentally determined melting points.

6. Conclusion

The liquidus projection, invariant equilibria and several vertical sections of the Bi–Cu–Pb ternary system were calculated using binary thermodynamic descriptions included in the COST 531 database. Phase transition temperatures of the alloys along three chosen vertical sections were measured using DSC. Predicted ternary eutectic reaction at 125 °C and ternary quasi-peritectic reaction at 183.5 °C were confirmed by the DSC results from this study. Calculated liquidus temperatures also show good agreement with experimentally determined liquidus temperatures. Further experimental study of this ternary system should be mainly focused on microstructure examination of equilibrated alloys in order to examine solubility of third element in binary phases. This would allow accurate thermodynamic modeling of Bi–Cu–Pb ternary system and possible introduction of ternary interaction parameters.

Acknowledgement

This work was supported by Ministry of Science of the Republic of Serbia (Project No. 142043).

References

[1] SGTE Unary Database, Version 4.4, Scientific Group Thermodata Europe, Teddington, UK, 2001.
[2] A.T. Dinsdale, A. Kroupa, J. Vízdal, J. Vrestal, A. Watson, A. Zemanova, COST 531 Database for Lead-free Solders, Ver. 3.0, 2008.
[3] N. Saunders, A.P. Miodownik, CALPHAD (A Comprehensive Guide), Elsevier, London, 1998.
[4] O. Redlich, A. Kister, Ind. Eng. Chem. 40 (1948) 345.
[5] Y.-M. Muggianu, M. Gambino, J.-P. Bros, J. Chim. Phys. 72 (1975) 83.
[6] J.-O. Andersson, A. Fernandez-Guillermet, M. Hillert, B. Jansson, B. Sundman, Acta Metall. 34 (1986) 437.
[7] M. Hillert, M. Jarl, CALPHAD 2 (1978) 227.
[8] G. Inden, Proceedings CALPHAD Conference, Dusseldorf III, 1976, pp. 1–4.
[9] G. Inden, Physica 103B (1981) 82.
[10] F.D. Murnaghan, Proc. Natl. Acad. Sci. U.S.A. 30 (1944) 244.
[11] A. Fernandez-Guillermet, P. Gustafson, M. Hillert, J. Phys. Chem. Solids 46 (1985) 1427–1429.
[12] A. Dinsdale, A. Watson, A. Kroupa, J. Vrestal, A. Zemanova, J. Vizdal, COST Action 531—Atlas of Lead Free Soldering, COST Office, Brussels, 2008, ISBN:978-80-86292r-r28-1.
[13] O. Teppo, J. Niemela, P. Taskinen, Report TKK-V-B50, University of Technology, Helsinki, 1989.
[14] D. Boa, I. Ansara, Thermochim. Acta 314 (1) (1998) 79–86.
[15] F.H. Hayes, H.-L. Lukas, G. Effenberg, G. Petzow, Z. Metallkde. 77 (11) (1986) 749–754.
[16] L.-S. Chang, B.B. Straumal, E. Rabkin, W. Gust, F. Sommer, J. Phase Equilib. 18 (1997) 128–135.
[17] U. Kattner, Bi–Cu–Pb System, Metallurgy Division of the Materials Science and Engineering Laboratory (MSEL) at the National Institute of Standards and Technology (NIST), 2003, Available at: http://www.metallurgy.nist.gov/phase/solder/bicupb.html.